ISSN No:-2456-2165

Effects of Viscous Dissipation on Double Diffusive Mixed Convective Nanofluid Flow along Inclined Plate in Porous Medium with Heat Generation

Md. Nasir Uddin[1], Tahmina Tahrim[2] and Md. Abdul Alim[3]
[1]Department of Mathematics, Bangladesh Army University of Engineering & Technology, Natore, Bangladesh
[2]Department of Computer Science and Engineering, Jagannath University, Dhaka, Bangladesh
[3]Department of Mathematics, Bangladesh University of Engineering and Technology, Dhaka, Bangladesh

Abstract:- With the inclusion of viscous dissipation, heat generation, and injection/suction effects, the mixed convective heat and mass transfer in aluminum oxide - water nanofluid flow along an inclined plate in a porous medium is numerically explored. Influential similarity transformations are used to convert the governing physical model of flow, which is expressed as a system of dimensional partial differential equations, into a set of dimensionless ordinary differential equations. The applicable Nachtsheim-Swigert approach and sixth-order Runge-Kutta integration process are used to numerically solve the relevant dimensionless ordinary differential equations and accompanying boundary conditions. The nanofluid flow's characteristics are evaluated for key parameters. The acquired numerical findings are reasonable and consistent with earlier accomplished numerical results from published literature. It is observed that as the Eckert number and the heat generation parameter grow, the velocity and temperature of the nanofluid flow field drop.

Keywords:- *Double diffusive; heat generation; inclined plate; mixed convection; porous medium; and viscous dissipation.*

I. INTRODUCTION

Due to numerous engineering applications and industrial processes, the impact of heat and mass transfer on nanofluid flow has become crucial in recent years. Important practical applications in the flow field through the medium of porous are things like drying of porous solids, petroleum industry, geothermal reservoirs, enriched oil recovery, boundary layer control in aerodynamics, food processing, design of various heat exchangers, as well as cooling of nuclear reactors and other things because of the involvement in not only heat transfer but also the mass transfer flow field and the nature of the process. Many scholars have been active in converting complex states into linear states because of their broad physical significance.

Heat transfer enhancement concerning boundary layer fluid flow for a different nanofluid flow passes through a vertical plate that has been studied with steady case via Rana and Bhargava [1], including with effects such as temperature dependent heat source/sink and an average Nusselt number that was found to diminish for different nanofluids. Non-Darcy steady mixed convection nanofluid flow through a horizontal plate has been explored via Rosca et al. [2] within a porous medium. Neglecting the mass transfer effect on the flow field, the velocity and temperature effects in regard to the field of flow have been presented graphically by Rosca et al. [2]. Due to the circumstance of steady, the mixed convection with regard to the nanofluid flow within the porous medium over the inclined plate has been explored by Rana et al. [3]. The standard thermo-physical properties of nanofluid have been ignored for analysis by them, and there is an opportunity to include these with the porous plate. Viscous nanofluid flow in the velocity and thermal boundary layer region has been reported by Kuppalapalle et al. [4]. There are various opportunities to extend Kuppalapalle et al. [4].

Ogunsola et al. [5] have focused on different impacts of heat as well as mass transfer characteristics with the assistance of mixed convective electrically accompanied fluid to flow inserted into a porous medium. Analytical together with numerical solutions of unsteady MHD natural convective fluid flow over and done with the vertical porous plate together with the impact based on thermal radiation as well as Hall current have been explored via Murthya et al. [6]. The efficient finite element and perturbation techniques have been applied by Murthya et al. [6] to solve reduced governing equations, and numerical results have been presented graphically. The impact based on the viscous dissipation in conjunction with radiative heat transfer in the boundary layer flow of considered nanofluid in regard to the presence of magnetic field past a rotating stretching surface has been examined and reported numerically via Wahiduzzaman et al. [7].

Hari et al. [8] investigated and analyzed MHD mixed convection occurring in fluid flow within a porous medium with radiation, including heat generation in the presence of chemical reaction effects. In the increasing magnetic field, the velocity profile overshoots adjacent to the plate surface and then convergences to the boundary that was found by them. Through porous media, MHD flow of nanofluid with the characteristic of heat including mass transfer has been reported along a stretching sheet via Reddy and Chamkha [9]. With the existence of viscous dissipation in cooperation with the thermal radiation effect, the analytical solution of the

steady two-dimensional flow with regard to the incompressible magnetohydrodynamic boundary layer flow based on the viscoelastic Jeffrey fluid in excess of the impermeable surface with heat generation/absorption has been studied by Sharma and Gupta [10]. The velocity reduces while temperature together with concentration enhances as per magnetic parameter increases which were found by them.

From the viewpoint of the significance with diffusion thermo and radiation absorption as well as chemical reaction effects in boundary layer flow, Vedavathia et al. [11] have examined a nanofluid of MHD free convective with simultaneous heat along with mass transfer through a semi-infinite vertical flat plate. In the existence of the dusty particle, the heat transfer characteristics using Maxwell fluid through a heated stretching sheet have been investigated by Gireesha et al. [12]. They discovered that dusty particles have a significant impact on the flow field of upper convected Maxwell fluid. Allowing for the MHD flow in regard to the nanofluid over a flat porous plate accompanied by injection/suction, heat absorption/generation, and viscous-Ohmic dissipation has been examined via Upreti et al. [13]. The authors demonstrated that the thickness in regard to the momentum boundary layer decays together with the growing values based on volume fraction for the sake of silver solid particles, even though the opposite tendency is detected in consideration of the thermal boundary layer. Considering the magnetic field as a special effect with viscous dissipation, Uddin et al. [14] have investigated the mixed convective fluid flow of nanofluid over and done with the inclined porous plate through a porous medium. There is an opportunity to extend this effort with the special properties of nanofluid flow.

The thought of the previously cited articles and their applications in various fields, such as numerous man-made industrial engineering and environmental fields, is of interest to deliberate and investigate the mixed convective flow based on nanofluid flow through over inclined plate under boundary conditions in a porous medium in the presence of viscous dissipation, heat generation, and injection/suction effects. The mentioned effects, together with the significant geometries, have not been studied yet to the best of the author's knowledge.

II. MATHEMATICAL ANALYSIS

In the presence of heat generation, mixed convection on nanofluid flow with the boundary conditions along the inclined plate in a porous medium is considered with the viscous dissipation effects. The base fluid is considered, such as water, whereas a nanoparticle is considered, such as aluminum oxide (Al_2O_3). Moreover, base fluid, as well as considered nanoparticles utilizing nanofluid, is in local thermal equilibrium. The physical model of the nanofluid flow in conjunction with the coordinate system of the considered nanofluid flow field is revealed in the Fig. 1.

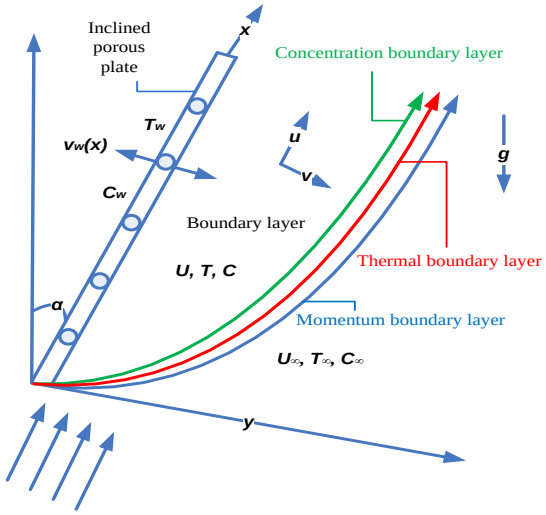

Fig. 1:- Diagram of the physical model together with coordinate system

For the current problem, the conservation law for mass is considered as

$$\frac{\partial u}{\partial x}+\frac{\partial v}{\partial y}=0 \qquad (1)$$

Moreover, the thermosphysical properties which are used for base fluid and nanoparticle are specified in the Table 1 as given by Ahmed et al. [15].

Particles	Thermophysical Properties				
	ρ (kg/m^3)	C_p (J/k g K)	k (W/m K)	β (1/K)	σ (S/m)
Water (H_2O)	997.1	417 9	0.613	21×10^{-5}	0.05
Copper (Cu)	8933	385	401	1.67×10^{-5}	5.96×10^{7}
Titanium Dioxide (TiO_2)	4250	686. 2	8.952 8	0.9×10^{-5}	1×10^{-12}
Aluminium Oxide (Al_2O_3)	3970	765	40	0.85×10^{-5}	1×10^{-10}

Table 1:- Thermophysical properties of base fluid and nanoparticle for the fluid flow

Under the present significant physical features of the nanofluid flow field, the revised system in regard to dimensional boundary layer equations of Pal and Mandal [16], as well as Bachok et al. [17] in terms of the expressions of basic conservation equations for momentum, is considered as

ISSN No:-2456-2165

$$u\frac{\partial u}{\partial x}+v\frac{\partial u}{\partial y}=\nu_{nf}\frac{\partial^2 u}{\partial y^2}+\frac{g}{\rho_{nf}}\left\{\begin{matrix}(\rho\beta_t)_{nf}(T-T_\infty)\\+(\rho\beta_c)_{nf}(C-C_\infty)\end{matrix}\right\}\cos\alpha$$

$$-\frac{\nu_{nf}}{k_{pp}}(u-U_\infty) \qquad (2)$$

while the energy as thermal accompanied by concentration equations can be expressed in Cartesian coordinates system such as

$$u\frac{\partial T}{\partial x}+v\frac{\partial T}{\partial y}=\alpha_{nf}\frac{\partial^2 T}{\partial y^2}$$

$$+\frac{1}{(\rho C_p)_{nf}}\left[\mu_{nf}\left\{u\frac{\partial^2 u}{\partial y^2}+(\frac{\partial u}{\partial y})^2\right\}+(T-T_\infty)Q_0\right] \qquad (3)$$

$$u\frac{\partial C}{\partial x}+v\frac{\partial C}{\partial y}=D\frac{\partial^2 C}{\partial y^2} \qquad (4)$$

wherever for the considered copper (Cu) - water nanofluid flow, ρ_{nf} is the density, α_{nf} is well read-out as the thermal diffusivity, $(\rho C_p)_{nf}$ is the heat capacitance and μ_{nf} is the viscosity. Furthermore, k_{pp} is the permeability regarding porous medium, Q_0 is the heat generation constant whereas D is the mass diffusivity.

For the nanofluid, effective dynamic viscosity was given via Brinkman [18] as

$$\mu_{nf}=\frac{\mu_{bf}}{(1-\phi)^{2.5}} \qquad (5)$$

where μ_{nf} is considered as dynamic viscosity of water base fluid and ϕ is considered as nanoparticle solid volume fraction.

The relation between physical quantities of base fluid and nanoparticle which were introduced by Abu-Nada [19] are defined as follows:

$$\rho_{nf}=(1-\phi)\rho_{bf}+\phi\rho_{np},$$

$$(\rho\beta_t)_{nf}=(1-\phi)(\rho\beta_t)_{bf}+\phi(\rho\beta_t)_{np},$$

$$(\rho\beta_c)_{nf}=(1-\phi)(\rho\beta_c)_{bf}+\phi(\rho\beta_c)_{np},$$

$$(\rho C_p)_{nf}=(1-\phi)(\rho C_p)_{bf}+\phi(\rho C_p)_{np},$$

$$\nu_{nf}=\frac{\mu_{nf}}{\rho_{nf}},\ \frac{K_{nf}}{K_{bf}}=\frac{(K_{np}+2K_{bf})-2\phi(K_{bf}-K_{np})}{(K_{np}+2K_{bf})+\phi(K_{bf}-K_{np})},$$

$$\text{and } \alpha_{nf}=\frac{K_{nf}}{(\rho C_p)_{nf}} \qquad (6)$$

wherever the subscripts in aforementioned equations *bf* and *np* symbolize namely base fluid and nanoparticle respectively.

In furthermore, the accompanying boundary situations depend on the existing nanofluid flow field through which the subsequent relations are as follows:

$$u=0,\ v=\pm v_w(x),\ T=T_w \text{ and } C=C_w \quad \text{at } y=0 \qquad (7)$$

$$u\to U_\infty,\ T\to T_\infty \text{ and } C\to C_\infty \quad \text{as } y\to\infty \qquad (8)$$

where, the subscripts w and ∞ denote wall and boundary layer edges respectively whereas the permeability of porous plate is as $v_w(x)$ which is for suction (< 0) or blowing (> 0).

Moreover, the equation of continuity is satisfied identically with the aid of using the succeeding well-known relations of stream function as considered in the form of

$$u=\frac{\partial\psi}{\partial y} \text{ and } v=-\frac{\partial\psi}{\partial x} \qquad (9)$$

The following significant dimensionless transformations are employed as follows to reduce the complexity of the anticipated nanofluid flow:

$$\eta=y\sqrt{\frac{U_\infty}{\nu_{bf}x}},\ \psi=\sqrt{\nu_{bf}xU_\infty}\ f(\eta),$$

$$\theta(\eta)=\frac{T-T_\infty}{T_w-T_\infty} \text{ and } s(\eta)=\frac{C-C_\infty}{C_w-C_\infty} \qquad (10)$$

and these transformations are familiarized by means of Cebeci and Bradshaw [20]. The velocity components of the nanofluid of Eqn. (9) using the Eqn. (10) are considered as

$$u=U_\infty f'(\eta) \text{ and } v=\frac{1}{2}\sqrt{\frac{\nu_{bf}U_\infty}{x}}\left[\eta f'(\eta)-f(\eta)\right] \qquad (11)$$

wherever the prime denotes the differentiation concerning η.

Using similarity transformations of Eqn. (10) in the Eqns. (2) – (4) including the associated boundary conditions in the Eqns. (7) – (8), the converted system of governing equations such as the momentum equation and the energy as well as concentration equations of the considered nanofluid flow are as below:

$$f'''+\phi_1\left\{\frac{1}{2}\phi_2 ff''+(\phi_3 Ri_t\,\theta+\phi_4 Ri_c\,s)\cos\alpha\right\}$$

$$+K(1-f')=0 \qquad (12)$$

$$\theta''+\frac{1}{2}\left(\frac{\Pr}{\phi_5}\right)\left\{\phi_6 f\theta'+\frac{2}{\phi_1}Ec\left(f'f'''+f''^2\right)+2\phi_5 Q\theta\right\}=0 \qquad (13)$$

$$s''+\frac{1}{2}Sc\,f\,s'=0 \qquad (14)$$

Moreover, the converted boundary conditions based on the corresponding transformed governing equations are obtained as

$$f = f_w,\ f' = 0,\ \theta = 1,\ s = 1,\ \text{at}\ \eta = 0 \tag{15}$$

$$f' \to 1,\ \theta \to 0\ \text{and}\ s \to 0\ \text{as}\ \eta \to \infty \tag{16}$$

In the previous-mentioned Eqn. (15), the coefficient obtained for wall mass transfer is considered as $f_w = -v_w(x)\sqrt{\dfrac{x}{\nu_{bf}U_\infty}}$ is the wall mass transfer coefficient as $f_w > 0$ for suction and $f_w < 0$ for injection or blowing.

However, the significant dimensionless physical parameters are considered as of defined by the Eqns. (12) – (14) with the conjunction of the following parameters:

$$Gr_t = \frac{g(\beta_t)_{bf}(T_w - T_\infty)x^3}{\nu_{bf}^{\ 2}},\ Gr_c = \frac{g(\beta_c)_{bf}(C_w - C_\infty)x^3}{\nu_{bf}^{\ 2}},$$

$$\mathrm{Re}_x = \frac{xU_\infty}{\nu_{bf}},\ Ri_t = \frac{Gr_t}{(\mathrm{Re}_x)^2},\ Ri_c = \frac{Gr_c}{(\mathrm{Re}_x)^2},\ K = \frac{x\nu_{bf}}{k_{pp}U_\infty},$$

$$\Pr = \frac{\nu_{bf}(\rho C_p)_{bf}}{K_{bf}},\ Ec = \frac{U_\infty^{\ 2}}{(C_p)_{bf}(T_w - T_\infty)},\ Sc = \frac{\nu_{bf}}{D},$$

$$Q = \frac{xQ_0}{(\rho C_p)_{bf}U_\infty},\ \phi_1 = (1-\phi)^{2.5},\ \phi_2 = (1-\phi) + \phi\frac{\rho_{np}}{\rho_{bf}},$$

$$\phi_3 = (1-\phi) + \phi\frac{(\rho\beta_t)_{np}}{(\rho\beta_t)_{bf}},\ \phi_4 = (1-\phi) + \phi\frac{(\rho\beta_c)_{np}}{(\rho\beta_c)_{bf}},$$

$$\phi_5 = \frac{K_{nf}}{K_{bf}}\ \text{and}\ \phi_6 = (1-\phi) + \phi\frac{(\rho C_p)_{np}}{(\rho C_p)_{bf}} \tag{17}$$

In the aforementioned Eqn. (18), Gr_t is the local thermal Grashof number, Gr_c is the local mass Grashof number, Re_x is the local Reynolds number, Ri_t is the local Richardson number of thermal, Ri_c is the local Richardson number of mass, Pr is the Prandtl number, K is specified as the parameter of permeability, Ec is indicated as Eckert number, Q is known as the heat generation parameter, Sc is directed as the Schmidt number whereas $\phi_i\,(i = 1,2,\cdots,6)$ are well thought-out as constants.

The significant physical features based on engineering awareness are like as a skin-friction coefficient C_f, local Nusselt number Nu_x in addition to local Sherwood number Sh. Under the circumstance, the well-known local skin-friction coefficient C_f and the local Nusselt Nu_x as well as the local Sherwood number Sh are denoted by way of

$$C_f = \frac{2}{\phi_1}(\mathrm{Re}_x)^{-\frac{1}{2}} f''(0) \tag{18}$$

$$Nu_x = -\phi_5(\mathrm{Re}_x)^{\frac{1}{2}}\theta'(0) \tag{19}$$

$$Sh = -(\mathrm{Re}_x)^{\frac{1}{2}} s'(0) \tag{20}$$

III. PROCEDURES OF NUMERICAL SOLUTIONS FOR THE CONSIDERED NANOFLUID FLOW

The system in regard to the obtained boundary value problem via means of Eqns. (12) - (14), as well as the corresponding boundary condition Eqns. (15) – (16) is solved with the help of the Nachtsheim and Swigert [21] approach that is applied for the sake of locating undefined initial conditions.

After finding the undefined initial conditions, the converted boundary value system is re-converted on the way to an initial value system in the form of an initial value problem. The obtained system is resolved numerically with the assistance of sixth order Runge-Kutta tactics. More than that, the convenient numerical approaches are considered by Nachtsheim and Swigert [21] as well as sixth order Runge-Kutta tactics through Al-Shimmary [22].

IV. COMPARISON OF NUMERICAL RESULTS

In order to obtain accuracy based on the present numerical results in regard to the nanofluid flow, comparisons are made in conjunction with the special effects on the subject of temperature, in addition to the velocity ratio parameter λ on velocity profiles.

The published results based on Bachok et al. [17] are matched with the current results in terms of verified by means of the authors in regard to copper (Cu) - water nanofluid flow using Prnadtl number as Pr = 6.2 more than that velocity ratio parameter as $\lambda = -0.4$ with the help of Fig. 2 as shown below. As a consequence, verified corresponding numerical results in regard to the first solution are established with excellent agreement. As a result, the favorable comparison is encouraged in the direction of expanding the numerical tactics of Nachtsheim and Swigert [21] based on the current work. The achieved numerical results in regard to nanofluid flow will be displayed graphically afterward in the following section rather than interpreted thereafter.

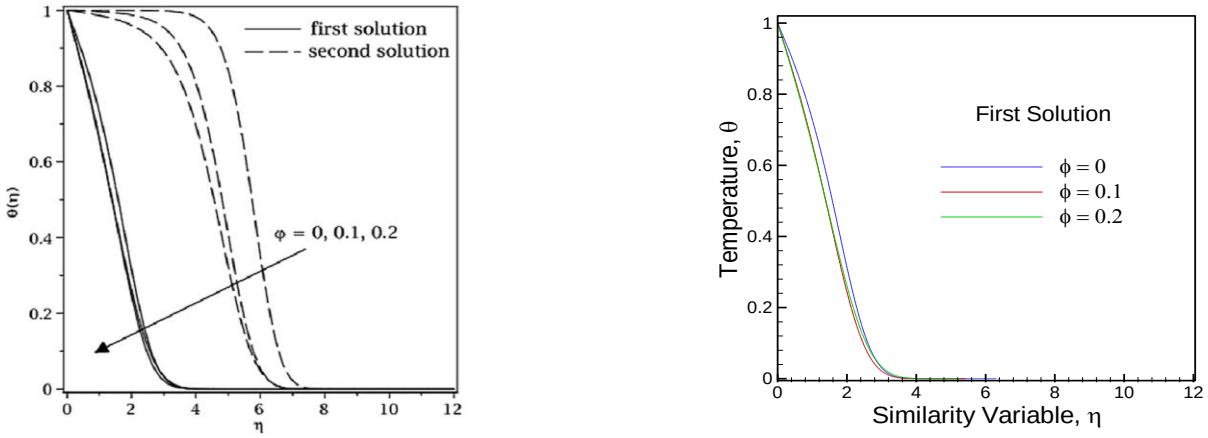

(a) (b)

Fig. 2: Comparison in regard to the first solution of temperature variation between (a) results of Bachok et al. [17] and (b) present results as verified of Bachok et al. [17] work for nanoparticle volume fraction ϕ with λ = - 0.4 and Pr = 6.2 using copper (Cu) - water nanofluid

V. RESULTS AND DISCUSSION OF SIGNIFICANT PARAMETERS

The physical significant numerical results of nondimensional parameters which are obtained based on aluminum oxide (Al_2O_3) – water nanofluid flow of heat in conjunction with mass transfers in terms of velocity, temperature together with concentration fields are worked out by using as f_w = 1.5, Pr = 6.2, Ri_t = 1, Ri_c = 1, K = 0.5, Ec = 0.5, Q = 0.5, ϕ = 0.03, $\alpha = 30^0$, Sc = 0.60 as well as U_∞/v = 1.0 and with the exception of formerly indicated. The nanofluid of the flow field is considered as the combination of aluminum oxide (Al_2O_3) and water such that water is considered by means of base fluid and aluminum oxide (Al_2O_3) is considered by means of nanoparticle together with thermophysical properties in Table 1.

Eckert number namely Ec is a measure regarding kinetic energy relative to enthalpy difference across the thermal boundary layer. The behavior regarding Eckert number Ec as Ec = 0, 1 and 2 on the aluminum oxide (Al_2O_3) – water nanofluid flow fields is revealed in Fig. 3. As in Fig. 3(a), it is realized that velocity regarding nanofluid flow declines to rise of Eckert number Ec. The thermal boundary layer breadth rises owing to reduction for Eckert number as detected from Fig. 3(b). The aforementioned represents the conversion regarding kinetic energy into internal energy by means of work done against viscous fluid stress. The negative Eckert number denotes the heating of the fluid. Accordingly, it is evidently noted that the temperature regarding nanofluid flow rises together with reduction of the magnitude of Eckert number. However, concentration regarding nanofluid flow increases with an increase of Ec as in Fig. 3(c). As to enhance of Eckert number Ec; wall shear stress regarding nanofluid flow reduces as a consequence skin friction coefficient C_f reduces whereas local Nusselt number Nu_x increases for aluminum oxide (Al_2O_3) – water nanofluid which are observed by Figs. 3(d) – 3(f). As shown on the Fig. 3(f), the local Sherwood number Sh reduces with the increase of Ec.

The influence of heat generation parameter Q as Q = 0, 0.5, and 1 on the aluminum oxide (Al_2O_3) – water nanofluid flow fields is shown in Fig. 4 while all other parameters remain unchanged. As observed in Fig. 4(a), the velocity as well as thermal boundary layers' thicknesses within the decreases with the increase in heat generation parameter. On the other hand, the concentration boundary layer thickness is observed as the insignificant effect with the increase in heat generation parameter in Fig. 4(c). The impact of heat generation parameter on the local skin friction coefficient, the local Nusselt number, and the local Sherwood number in the boundary layer against the streamwise distance x for aluminum oxide (Al_2O_3) – water nanofluid flow are shown in Figs. 4(d) – 4(f). As observation in Figs. 4(d) – 4(f), it is noted that the local skin friction coefficient decreases whereas the local Nusselt number increases due to increase in the heat generation parameter, and however the local Sherwood number changes insignificantly.

The impacts of different types of nanofluids on the boundary layer flow fields with the assistance of velocity in conjunction with temperature as well as concentration are exposed with the help of Figs. 5(a) – 5(f). The different types of nanofluids are copper (Cu) – water, titanium dioxide (TiO_2) – water, and aluminum oxide (Al_2O_3) – water. It is observed in Fig. 5(a) that the velocity of the copper (Cu) – water nanofluid flow is higher than the titanium dioxide (TiO_2) – water and aluminum oxide (Al_2O_3) – water near the wall and then converse to the boundary condition. On the other hand, the temperature of the copper (Cu) – water nanofluid flow is lower than the titanium dioxide (TiO_2) – water and aluminum oxide (Al_2O_3) – water near the wall and then higher in the next and then converse to the boundary condition as seen in Fig. 5(b). Moreover, the copper (Cu) – water as well as titanium dioxide (TiO_2) – water and aluminum oxide (Al_2O_3) – water nanofluid flows are shown insignificant behavior for concentration as observed in Fig. 5(c). Consequently, the local skin friction coefficient C_f is higher than for copper (Cu) – water nanofluid flow as comparing with the titanium dioxide (TiO_2) – water and aluminum oxide (Al_2O_3) – water while local Nusselt number

ISSN No:-2456-2165

Nu_x and local Sherwood number *Sh* are observed as the insignificant effect due to copper (Cu) – water nanofluid flow as comparing with the titanium dioxide (TiO_2) – water and aluminum oxide (Al_2O_3) – water as observed in Figs. 5(d) – 5(f).

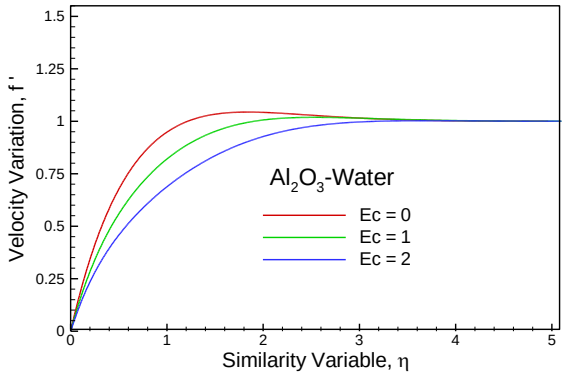

Fig. 3(a):- Velocity variation due to Eckert number *Ec*

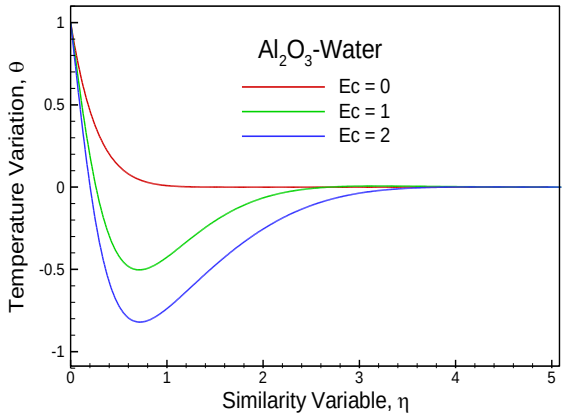

Fig. 3(b):- Temperature variation due to Eckert number *Ec*

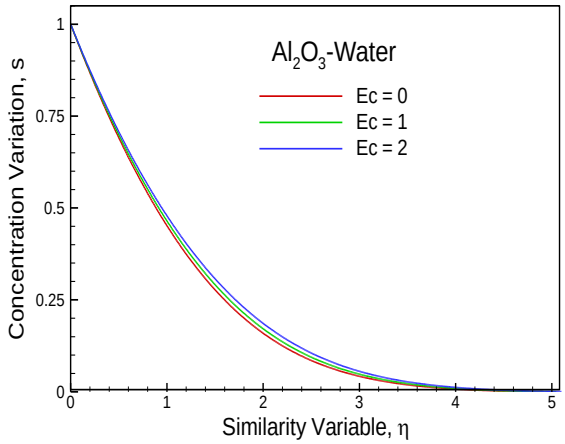

Fig. 3(c):- Concentration variation due to Eckert number *Ec*

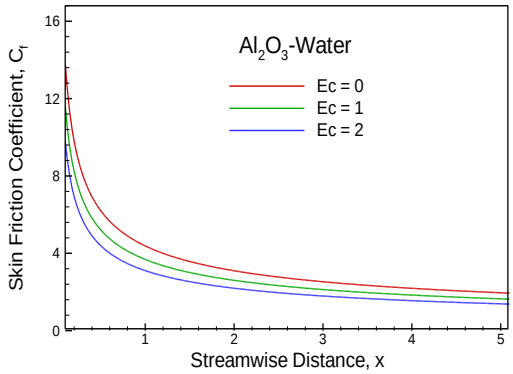

Fig. 3(d):- Variation of skin friction coefficient C_f in regard to the Eckert number *Ec*

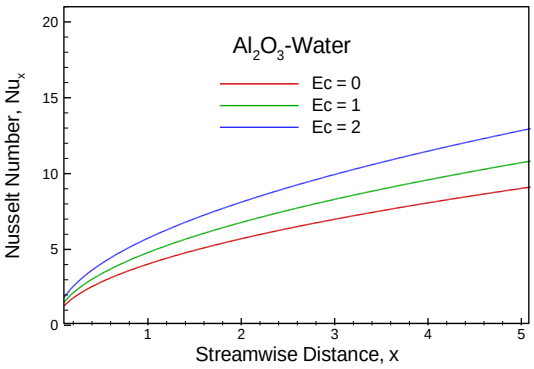

Fig. 3(e):- Variation of local Nusselt number Nu_x in regard to the Eckert number *Ec*

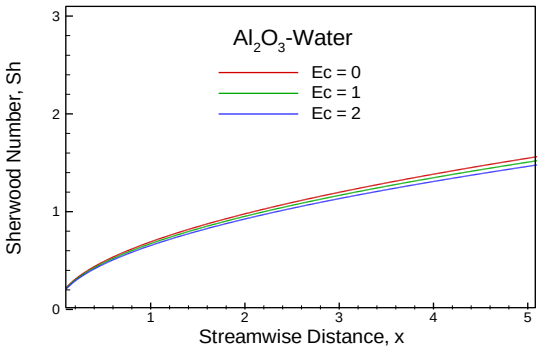

Fig. 3(f):- Variation of local Sherwood number *Sh* in regard to the Eckert number *Ec*

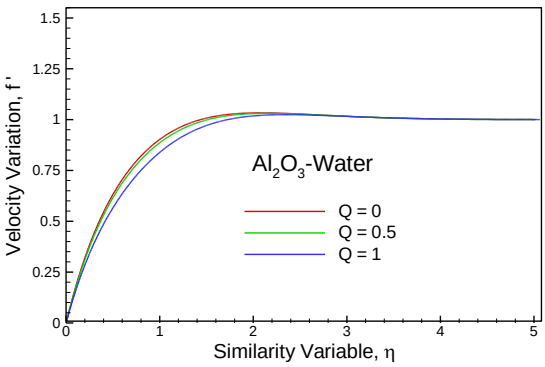

Fig. 4(a):- Velocity variation due to heat generation *Q*

ISSN No:-2456-2165

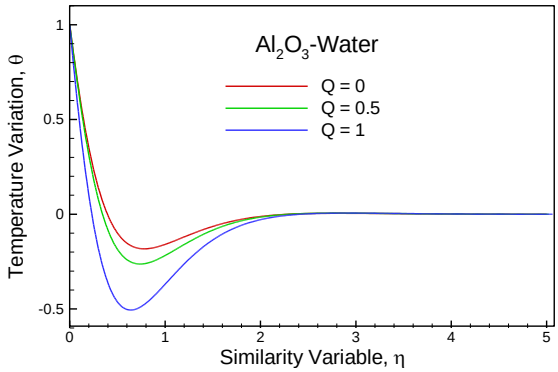

Fig. 4(b):- Temperature variation due to heat generation Q

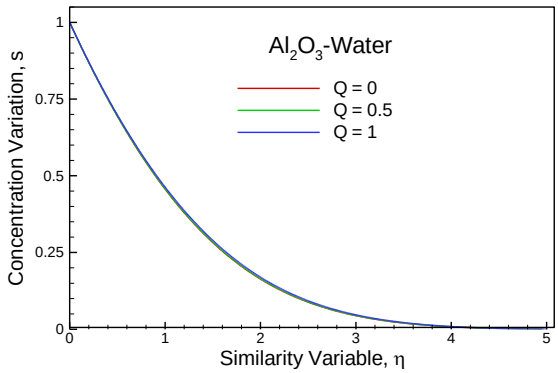

Fig. 4(c):- Concentration variation due to heat generation Q

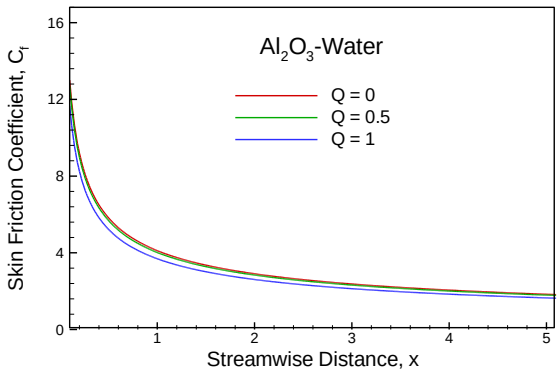

Fig. 4(d):- Variation of skin friction coefficient C_f in regard to the heat generation Q

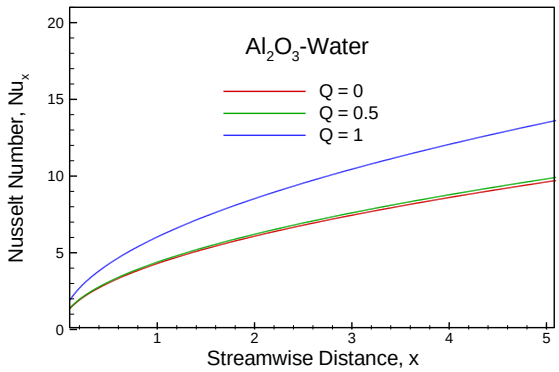

Fig. 4(e):- Variation of local Nusselt number Nu_x in regard to the heat generation Q

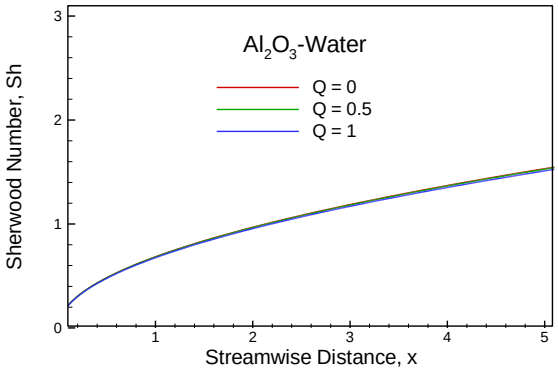

Fig. 4(f):- Variation of local Sherwood number Sh in regard to the heat generation Q

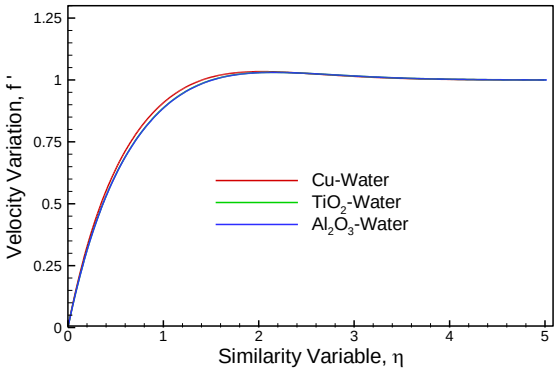

Fig. 5(a):- Velocity variation due to various nanofluids

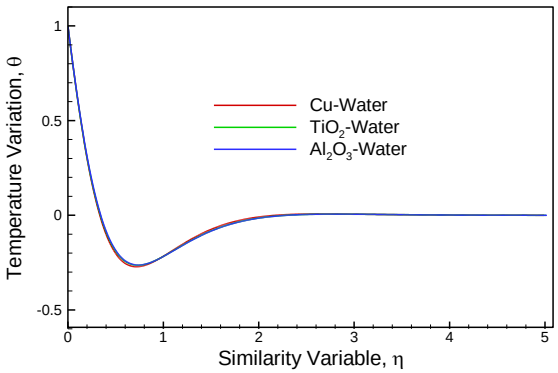

Fig. 5(b):- Temperature variation due to various nanofluids

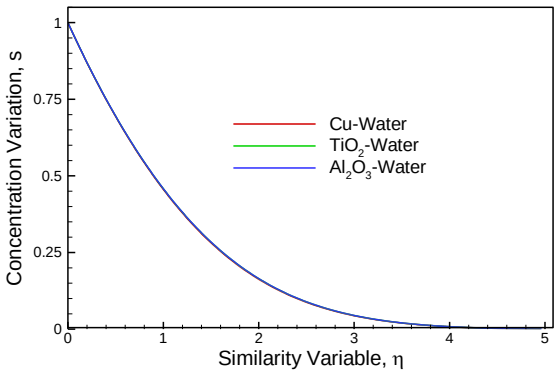

Fig. 5(c):- Concentration variation due to various nanofluids

ISSN No:-2456-2165

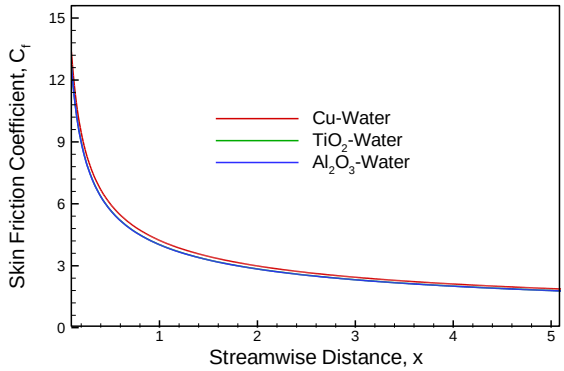

Fig. 5(d):- Variation of skin friction coefficient C_f in regard to various nanofluids

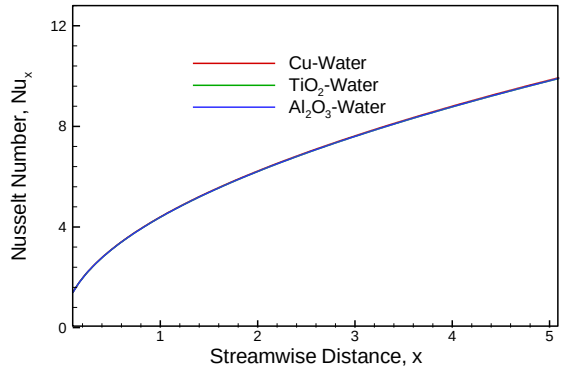

Fig. 5(e):- Variation of local Nusselt number Nu_x in regard to various nanofluids

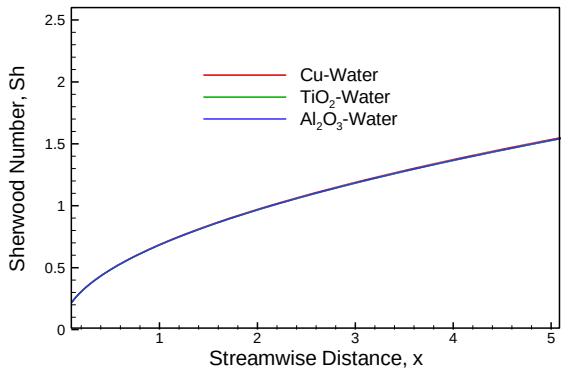

Fig. 5(f):- Variation of local Sherwood number *Sh* in regard to various nanofluids

VI. CONCLUSIONS BASED ON THE NUMERICAL OUTCOMES

For the sake of presence as concerns of viscous dissipation, mixed convective nanofluid of aluminum oxide (Al_2O_3) - water nanofluid flow in conjunction with heat generation effects along inclined plate through the medium of porous is examined numerically. Moreover, the considered governing equations in regard to nanofluid flow are transformed on the way to non-linear differential equations with the help of similarity transformation, and transformed governing equations related to boundary layer flow field are resolved numerically by means of Runge – Kutta process through the technique of shooting of Nachtsheim and Swigert [21].

The obtained numerical results are compared to existing works previously reported by Bachok et al. [17]. More than that, comparatively, a pleasing assessment is reached. The numerical outcomes based on Eckert number *Ec* and heat generation parameter *Q* for the aluminum oxide (Al_2O_3) – water nanofluid flow are presented sketchily and deliberated as well as for different nanofluid flows. The leading outcomes of the nanofluid flow can be elaborated as follows:

- The corresponding boundary layers' thicknesses of the velocity and temperature of the nanofluid flow field decrease on account of the increase of the Eckert number *Ec* while the concentration of the flow field increases with an increase of the Eckert number *Ec*. Under the obtained circumstances, the skin friction coefficient C_f, and local Sherwood number *Sh* based on nanofluid flow show decreasing behavior, whereas local Nusselt number Nu_x shows decreasing behavior for the sake of increasing values of Eckert number *Ec*.
- Increasing values of the heat generation parameter *Q* lead to a decrease in both the velocity and temperature in the flow field, and consequently decrease the local skin friction coefficient C_f but increase the local Nusselt number Nu_x. However, as the heat generation parameter *Q* is increased, the concentration and the local Sherwood number *Sh* change insignificantly.
- The velocity of the copper (Cu) – water nanofluid flow is higher than the titanium dioxide (TiO_2) – water and aluminum oxide (Al_2O_3) – water near the wall and then converses to the boundary condition, while the temperature of the copper (Cu) – water nanofluid flow is lower than the titanium dioxide (TiO2) – water and aluminum oxide (Al2O3) – water near the wall and then higher in the next and then converses to the boundary condition, but concentration shows insignificant behavior for the nanofluids. More than that, the local skin friction coefficient C_f is higher than while local Nusselt number Nu_x and local Sherwood number *Sh* are observed as the insignificant effect due to copper (Cu) – water nanofluid flow as comparing with the titanium dioxide (TiO_2) – water and aluminum oxide (Al_2O_3) – water.

REFERENCES

[1]. Rana, P. and Bhargava, R., "Numerical Study of Heat Transfer Enhancement in Mixed Convection Flow along a Vertical Plate with Heat Source/Sink Utilizing Nanofluids", *Commun Nonlinear Sci Number Simulate*, vo. 16, pp. 4318-4334, 2011.

[2]. Rosca, A.V., Rosca, N. C., Grosan, T. and Pop, I., "Non-Darcy Mixed Convection from a Horizontal Plate Embedded in a Nanofluid Saturated Porous Media", *International Communications of Heat and Mass Transfer*, vol. 39, pp. 1080-1085, 2012.

[3]. Rana, P., Bhargava, R. and Beg, O. A., "Numerical Solution for Mixed Convection Boundary Layer Flow of a Nanofluid along an Inclined Plate Embedded in a Porous Medium", *Computer and Mathematics with Applications*, vol. 64, pp. 2816-2832, 2012.

[4]. Kuppalapalle, V., Vinayaka, P. K. and Chiu-On, N., "The Effect of Variable Viscosity on the Flow and Heat Transfer of a Viscous Ag-Water and Cu-Water Nanofluids", *Journal of Hydrodynamics*, vol. 25, issue 1, pp. 1-9, 2013.
[5]. Ogunsola, A. W., Olanrewaju, P. O., Alao, F. I., Osinowo, R. and Fenuga, O. J., "Effects of Thermal Diffusion and Diffusion Thermo on MHD Combined Convection and Mass Transfer Past a Vertical Porous Plate Embedded in a Porous Medium with Heat Generation, Thermal Radiation, nth Order Chemical Reaction and Viscous Dissipation", *Journal of Science and Engineering Research*, vol. 1 (1), pp. 01-19, 2014.
[6]. Murthya, M. V. R., Raju, R. S. and Rao, J. A., "Heat and Mass Transfer Effects on MHD Natural Convection Flow Past an Infinite Vertical Porous Plate with Thermal Radiation and Hall Current", *Procedia Engineering*, vol. 127, pp. 1330-1337, 2015.
[7]. Wahiduzzaman, M., Khan, M. S., Biswas, P., Karim, I. and Uddin, M. S., "Viscous Dissipation and Radiation Effects on MHD Boundary Layer Flow of a Nanofluid Past a Rotating Stretching Sheet", *Applied Mathematics*, vol. 6, pp. 547-567, 2015.
[8]. Hari, N., Sivasankaran, S., Bhuvaneswari, M. and Siri, Z., "Effects of Chemical Reaction on MHD Mixed Convection Stagnation Point Flow Toward a Vertical Plate in a Porous Medium with Radiation and Heat Generation", *Journal of Physics: Conference Series*, vol. 662, pp. 012-024, 2015.
[9]. Reddy, P. S. and Chamkha, A. J., "Soret and Dufour Effects on MHD Convective Flow of Al_2O_3-Water and Tio_2-Water Nanofluids Past a Stretching Sheet in Porous Media with Heat Generation/Absorption," *Advanced Power Technology*, vol. 27, pp. 1207-1218, 2016.
[10]. Sharma, K. and Gupta, S., "Viscous Dissipation and Thermal Radiation Effects in MHD Flow of Jeffrey Nanofluid through Impermeable Surface with Heat Generation/Absorption", *Nonlinear Engineering*, vol. 6 (2), pp. 153–166, 2017.
[11]. Vedavathia, N., Dharmaiahb, G., Balamuruganc, K. S. and Prakashd, J., "Heat Transfer on MHD Nanofluid Flow over a Semi-Infinite Flat Plate Embedded in a Porous Medium with Radiation Absorption, Heat Source and Diffusion Thermo Effect", *Frontiers in Heat and Mass Transfer*, vol. 9 (38), pp. 1-08, 2017.
[12]. Gireesha, B. J., Mahanthesh, B., Gorla, R. S. R. and Krupalakshmi, K. L., "Mixed convection two-phase flow of Maxwell fluid under the influence of non-linear thermal radiation, non-uniform heat source/sink and fliud-particle suspension", *Ain Shams Engineering Journal*, vol. 09, issue 4, pp. 735-746, December 2018.
[13]. Upreti, H., Pandey, A. K. and Kumar, M., "MHD Flow of Ag-Water Nanofluid over a Flat Porous Plate with Viscous-Ohmic Dissipation, Suction/Injection and Heat Generation/Absorption", *Alexandria Engineering Journal*, vol. 57, pp. 1839-1847, 2018.
[14]. Uddin, M. N., Alim, A. A., and Rahman, M. M., "MHD Effects on Mixed Convective Nanofluid Flow with Viscous Dissipation in Surrounding Porous Medium", *Journal of Applied Mathematics and Physics*, vol. 7, pp. 968-982, 2019.
[15]. Ahmed, S. E., Hussein, A. K., Mansour, M. A., Raizah, Z. A. and Zhang, X., "MHD Mixed Convection in Trapezoidal Enclosures Filled with Micropolar Nanofluids", Nanoscience and Technology: An International Journal, vol. 9(4), pp. 343-372, 2018.
[16]. Pal, D. and Mandal, G., "Influence of Thermal Radiation on Mixed Convection Heat and Mass Transfer Stagnation-Point Flow in Nanofluids Over Stretching/Shrinking Sheet in a Porous Medium with Chemical Reaction", *Nuclear Engineering and Design*, vol. 273, pp. 644-652, 2014.
[17]. Bachok, N., Ishak, A. and Pop, I., "Flow and Heat Transfer Characteristic on a Moving Plate in a Nanofluid", *International Journal of Heat and Mass Transfer*, vol. 55, pp. 642-648, 2012.
[18]. Brinkman, H. C., "The Viscosity of Concentrated Suspension and Solution", *The Journal of Chemical Physics*, vol. 20, pp. 571-581, 1952.
[19]. Abu-Nada, E., "Application of Nanofluids for Heat Transfer Enhancement of Separated Floes Encountered in a Backward Facing Step", *International Journal of Heat and Fluid Flow*, vol. 29, pp. 242-249, 2008.
[20]. Cebeci, T. and Bradshaw, P., "Physical and Computational Aspects of Convective Heat Transfer, *Springer*, New York, 1984.
[21]. Nachtsheim, P. R. and Swigert, P., "Satisfaction of Asymptotic Boundary Conditions in Numerical Solution of Systems of Nonlinear Equations of Boundary-Layer Type", *NASA TND* 3004, 1965.
[22]. Al-Shimmary, A. F. A., "Solving Initial Value Problem using Runge-Kutta 6th Order Method", *ARPN Journal of Engineering and Applied Sciences*, vol. 12 (13), pp. 3953-3961, July 2017.